Electronic Supplementary Material (ESI) for Molecular Systems Design & Engineering.

Evaluating the CO_2 capture performance of a "phase-change" metal-organic framework in a pressure-vacuum swing adsorption process

David Danaci,[1*] Elena Pulidori,[2] Luca Bernazzani,[2] Camille Petit,[1] Marco Taddei[2,3*]

[1] *Barrer Centre, Department of Chemical Engineering, Imperial College London, London, SW7 2AZ, UK. E-mail: david.danaci@imperial.ac.uk*

[2] *Dipartimento di Chimica e Chimica Industriale, Unità di Ricerca INSTM, Università di Pisa, Via Giuseppe Moruzzi 13, 56124 Pisa, Italy. Email: marco.taddei@unipi.it*

[3] *Energy Safety Research Institute, Swansea University, Fabian Way, Swansea, SA1 8EN UK*

ELECTRONIC SUPPLEMENTARY INFORMATION

1. Supplementary figures

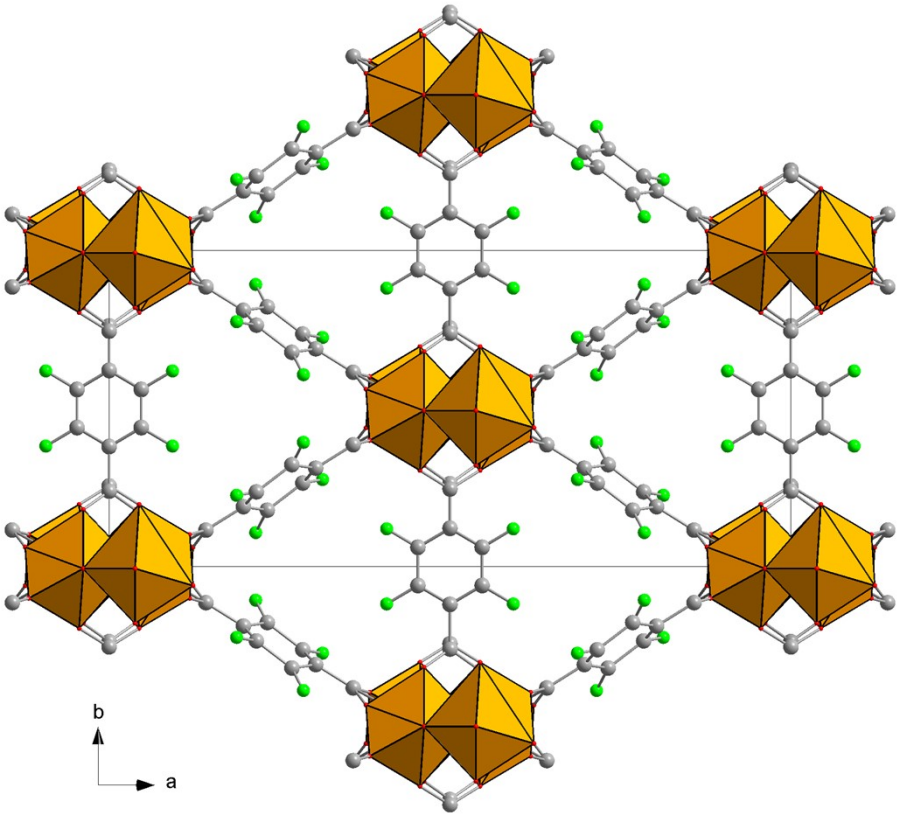

Figure S1. Crystal structure of F4_MIL-140A(Ce) viewed along the crystallographic *c* axis. Colour code: Ce, orange; F, green; C, grey; O, red; H_2O, blue.

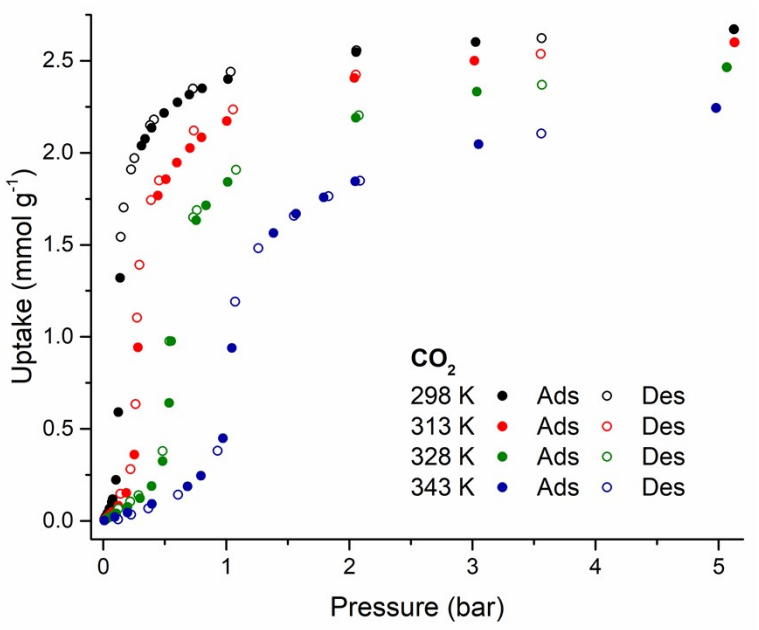

Figure S2. CO_2 adsorption (filled circles) and desorption (empty circles) isotherms for F4_MIL-140A(Ce) collected at 298 K (black), 313 K (red), 328 K (green) and 343 K (blue) in the 0-5 bar pressure range.

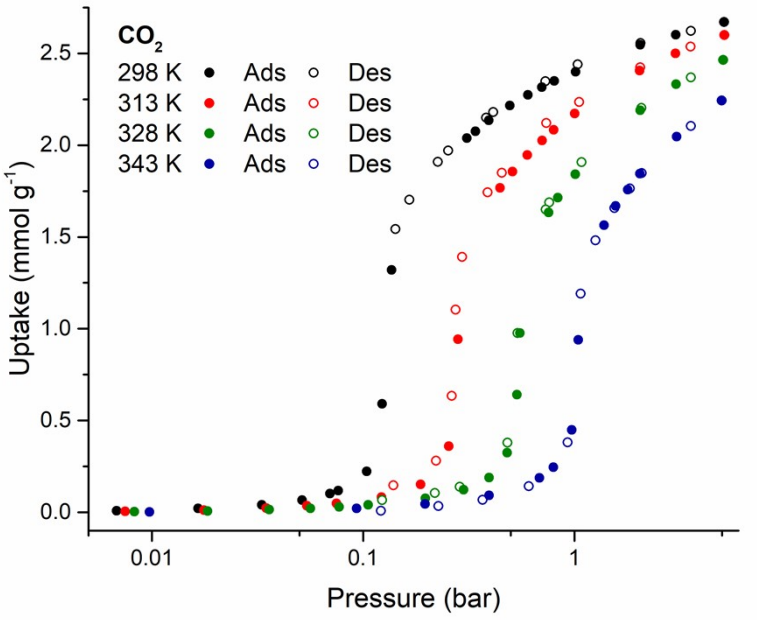

Figure S3. CO_2 adsorption (filled circles) and desorption (empty circles) isotherms for F4_MIL-140A(Ce) collected at 298 K (black), 313 K (red), 328 K (green) and 343 K (blue) in the 0-5 bar pressure range. The *x* axis is displayed in logarithmic scale.

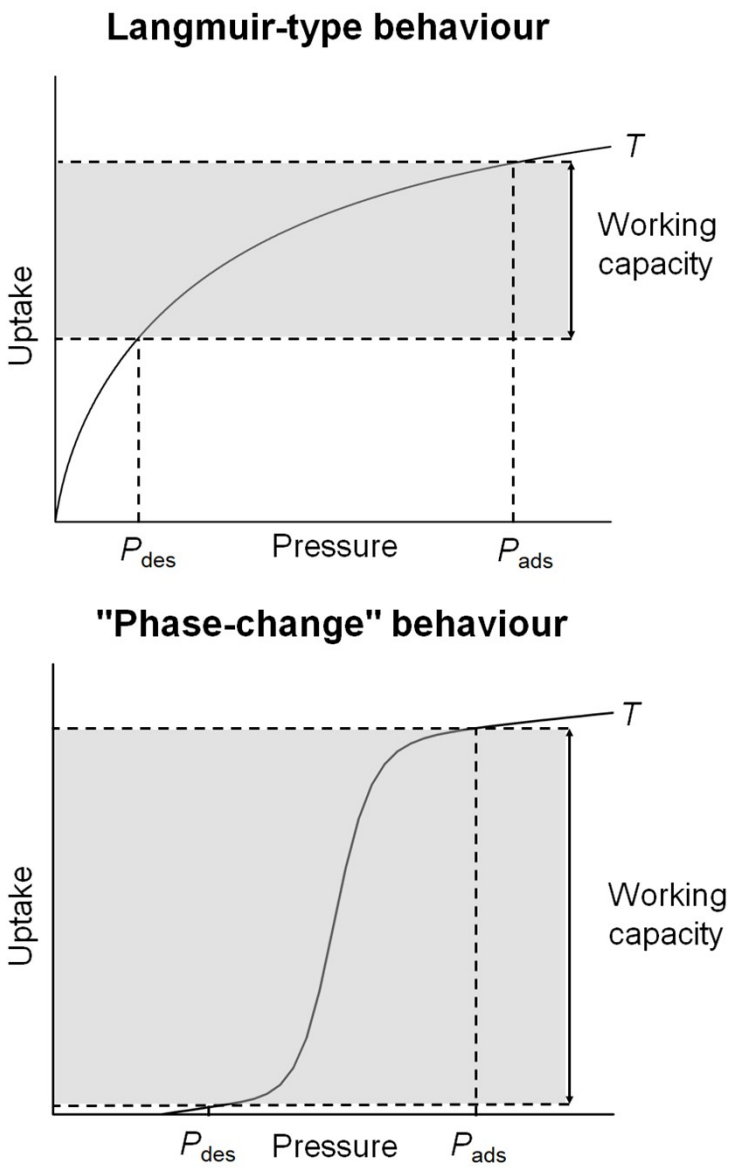

Figure S4. Ideal working capacity achievable with a Langmuir-type adsorbent (top) and a phase-change adsorbent (bottom) in an isothermal PVSA process.

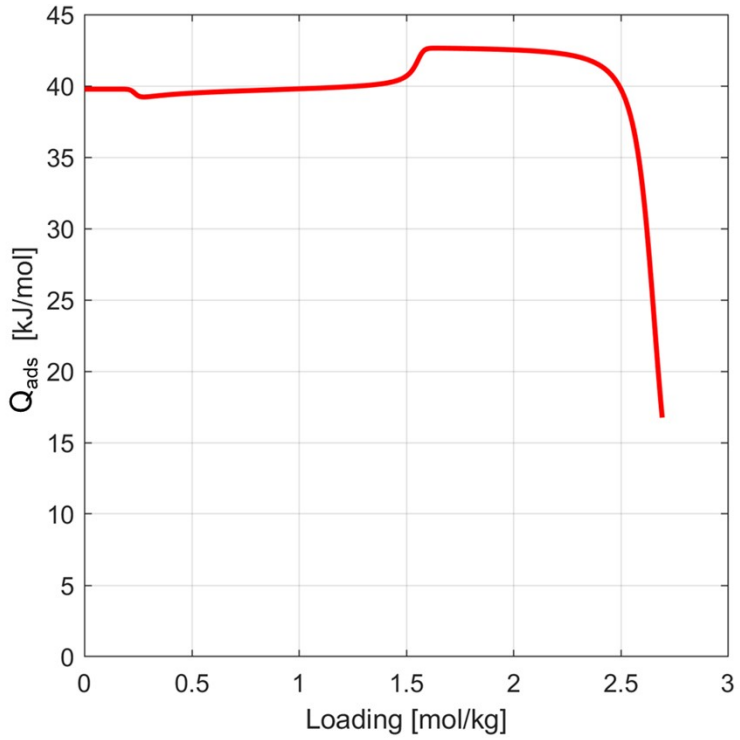

Figure S5. Isosteric heat of CO_2 adsorption (Q_{ads}) for F4_MIL-140A(Ce) versus the loading.

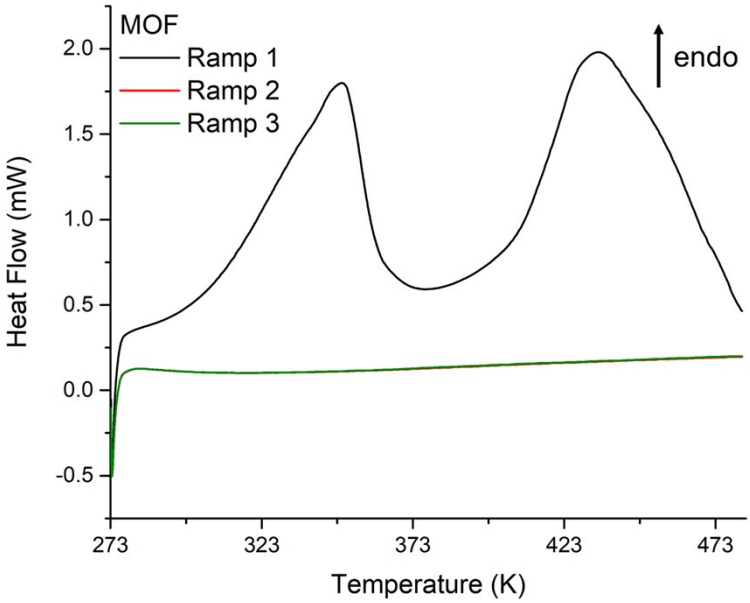

Figure S6. Typical DSC profile for F4_MIL-140A(Ce). During the first heating ramp, two endothermic events are observed, associated with the loss of weakly physisorbed water (below 373 K) and coordinated water (above 373 K), respectively. The second and third ramp are superimposed and no endothermic events are observed, confirming that all the adsorbed water has been removed during the first heating ramp.

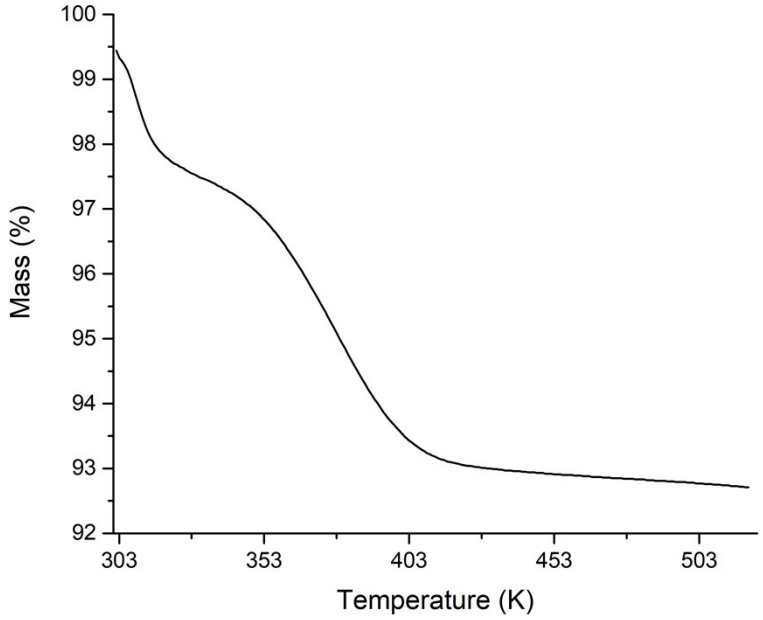

Figure S7. Thermogravimetric curve of F4_MIL-140A(Ce) under N_2 atmosphere.

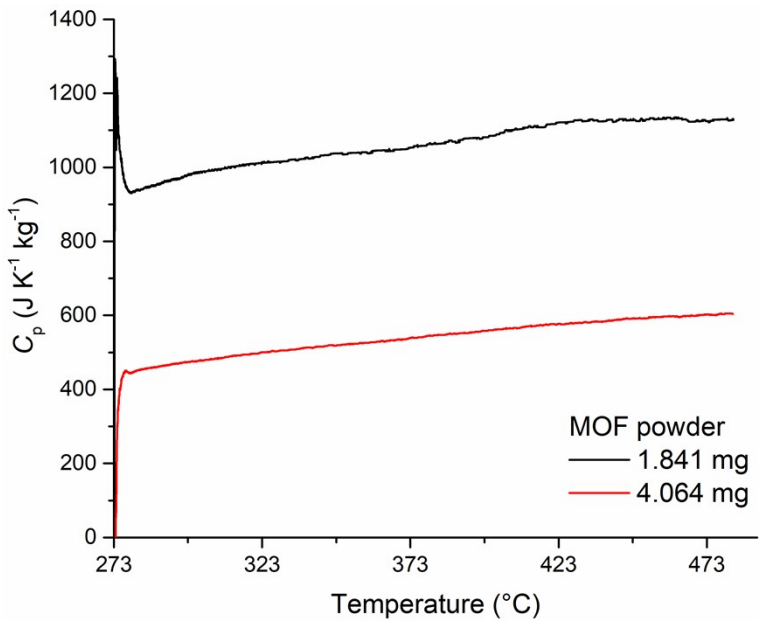

Figure S8. Comparison between the C_p values obtained for 1.841 mg (black) and 4.064 mg (red) of F4_MIL-140A(Ce) powder.

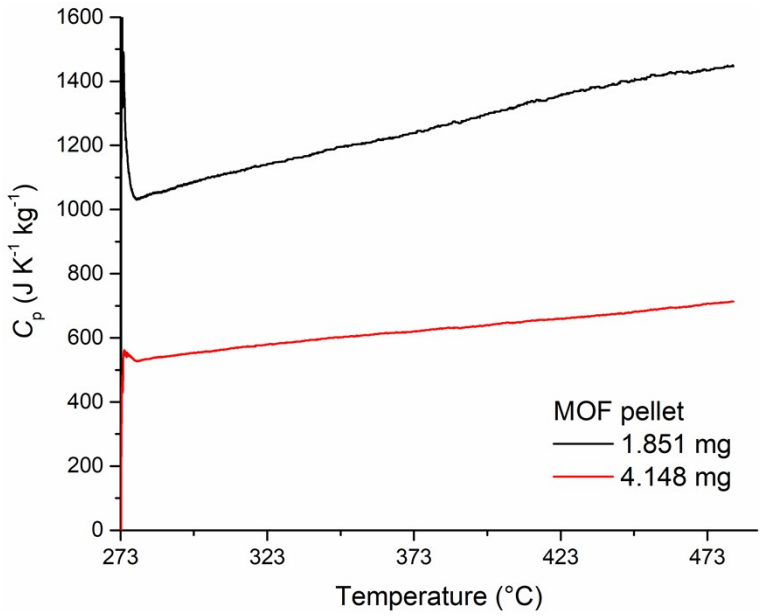

Figure S9. Comparison between the C_p values obtained for 1.851 mg (black) and 4.148 mg (red) of F4_MIL-140A(Ce) powder compressed into a thin pellet.

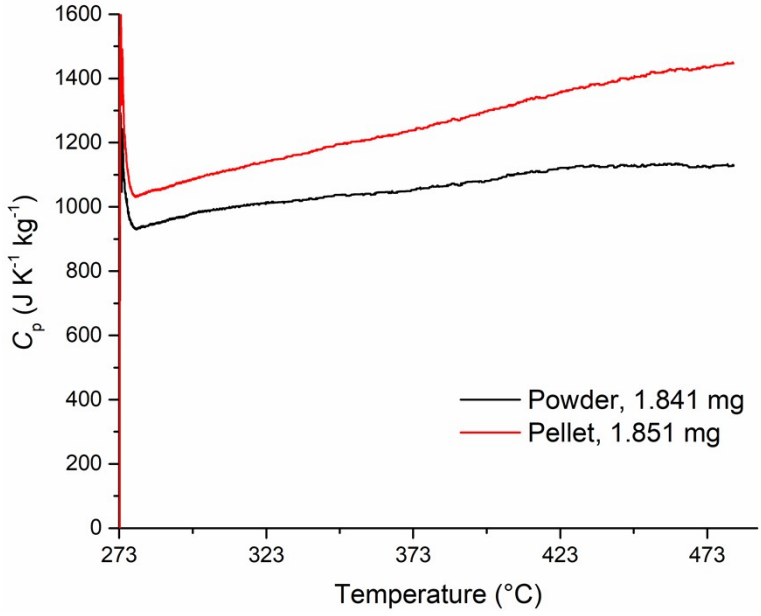

Figure S10. Comparison between the C_p values obtained for 1.841 mg of F4_MIL-140A(Ce) free-flowing powder (black) and 1.851 mg compressed into a thin pellet (red).

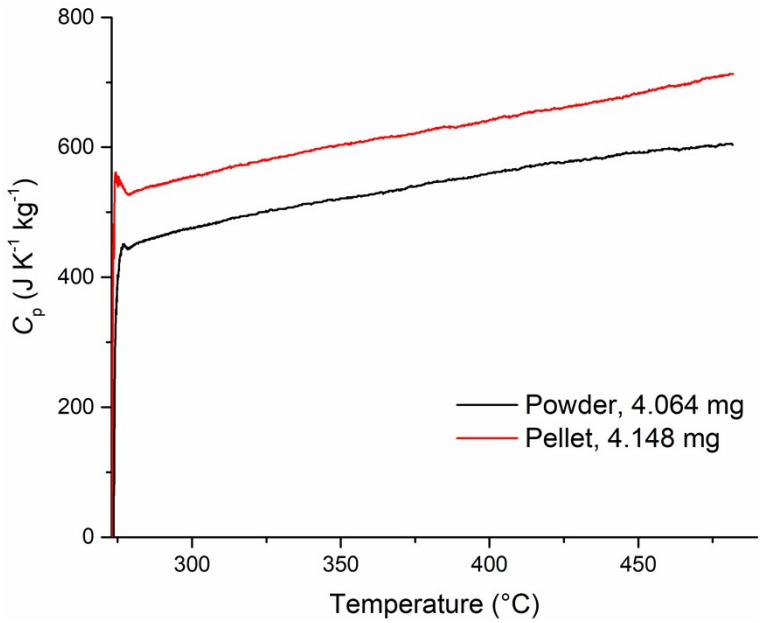

Figure S11. Comparison between the C_p values obtained for 4.064 mg of F4_MIL-140A(Ce) free-flowing powder (black) and 4.148 mg compressed into a thin pellet (red).

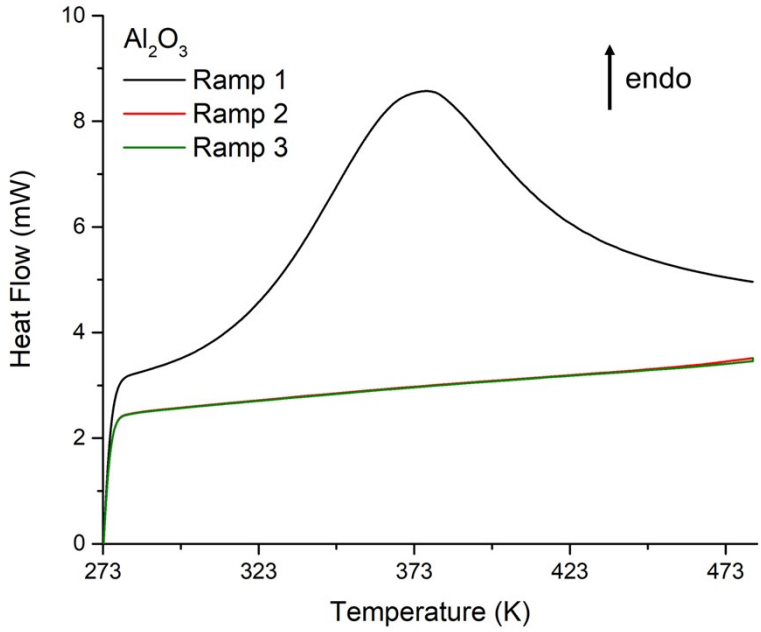

Figure S12. Typical DSC profile for activated alumina. During the first heating ramp, one endothermic event is observed, associated with the loss of surface adsorbed water. The second and third ramp are superimposed and no endothermic events are observed, confirming that all the adsorbed water has been removed during the first heating ramp.

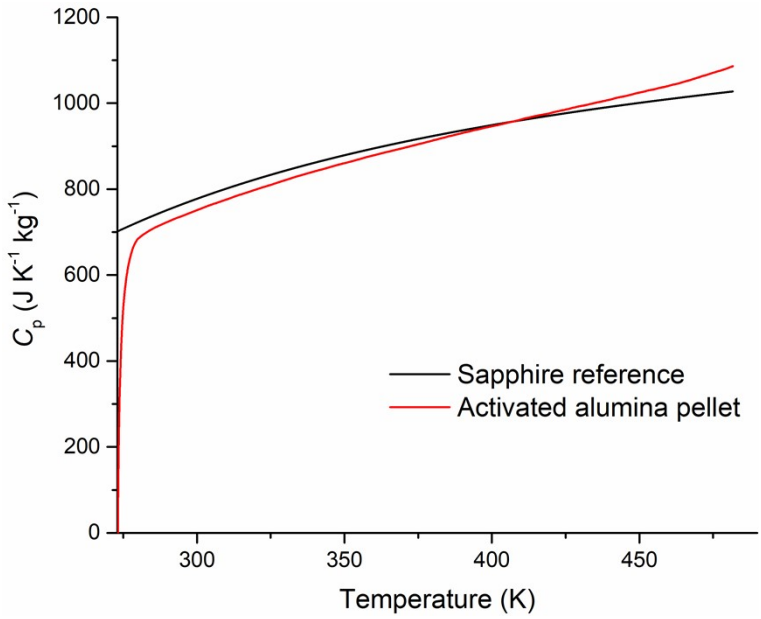

Figure S13. Comparison between the C_p values obtained for the reference sapphire crystal (black) and activated alumina compressed into a pellet (red).

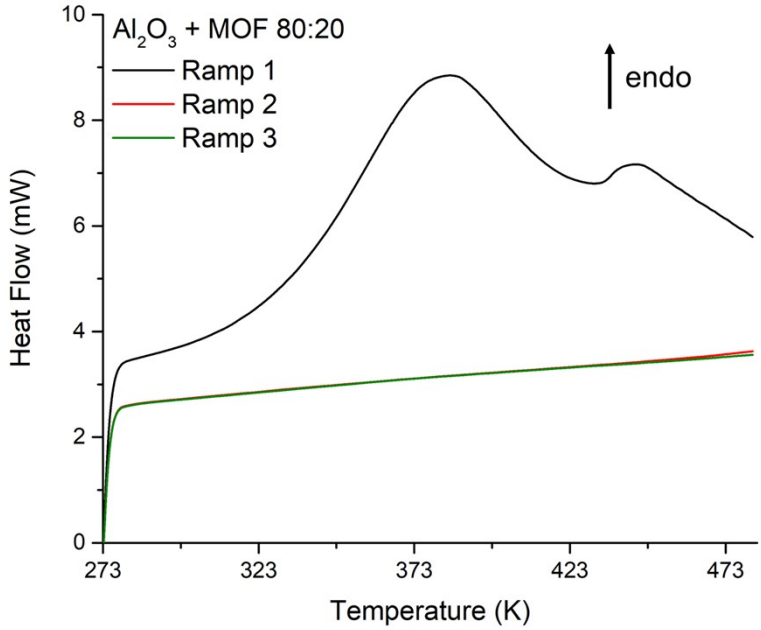

Figure S14. DSC profile for the composite pellet prepared mixing activated alumina and F4_MIL-140A(Ce) in a 80:20 wt% ratio. During the first heating ramp, two endothermic events are observed, associated with the loss of surface adsorbed water from alumina (DSC curve peaking at 383 K) and coordinated water from F4_MIL-140A(Ce) (DSC curve peaking at 443 K), respectively. The second and third ramp are superimposed and no endothermic events are observed, confirming that all the adsorbed water has been removed during the first heating ramp.

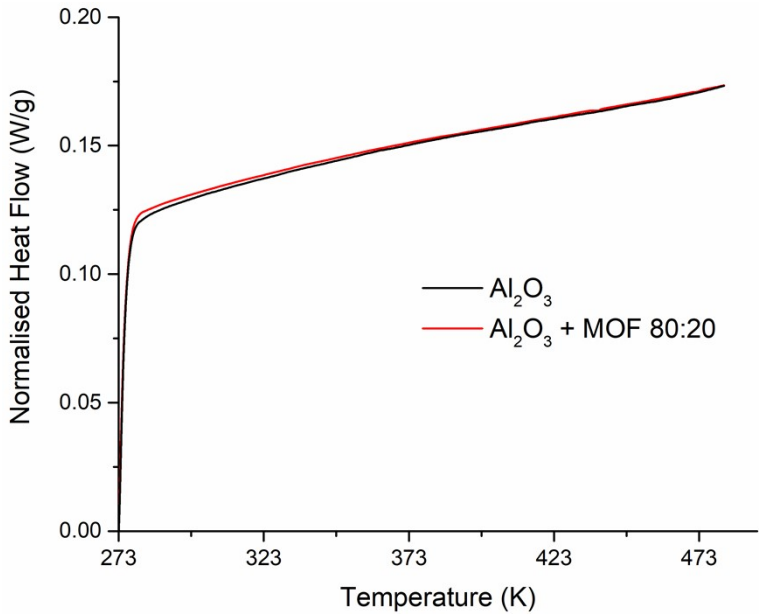

Figure S15. Comparison between the normalised heat flow values obtained for activated alumina compressed into a pellet (black) and a composite pellet prepared mixing activated alumina and F4_MIL-140A(Ce) in a 80:20 wt% ratio (red).

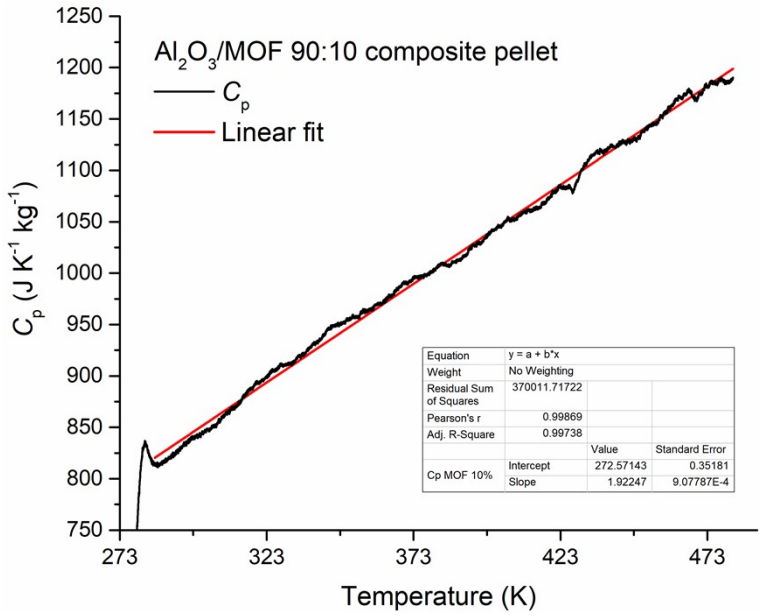

Figure S16. Linear fitting in the 285-480 K temperature range (red) of the C_p curve for the composite pellet prepared mixing activated alumina and F4_MIL-140A(Ce) in a 90:10 wt% ratio (black).

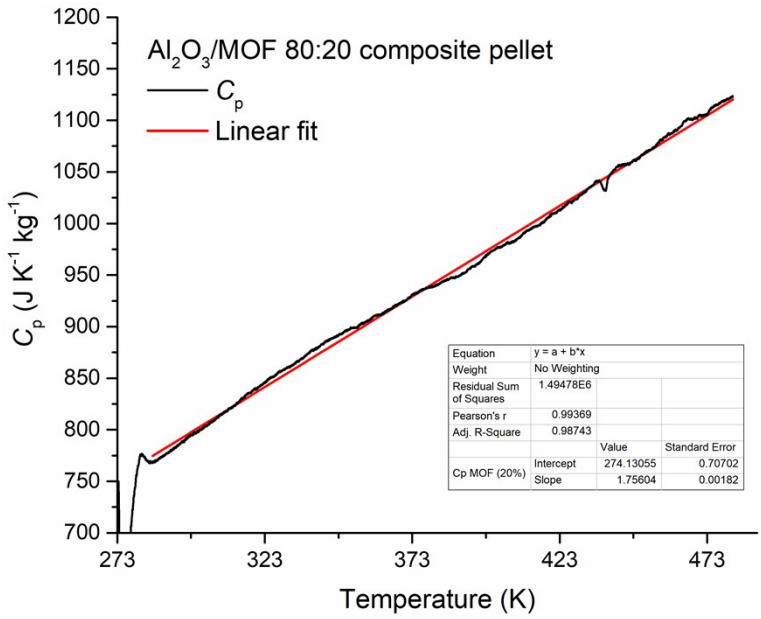

Figure S17. Linear fitting in the 285-480 K temperature range (red) of the C_p curve for the composite pellet prepared mixing activated alumina and F4_MIL-140A(Ce) in a 80:20 wt% ratio (black).

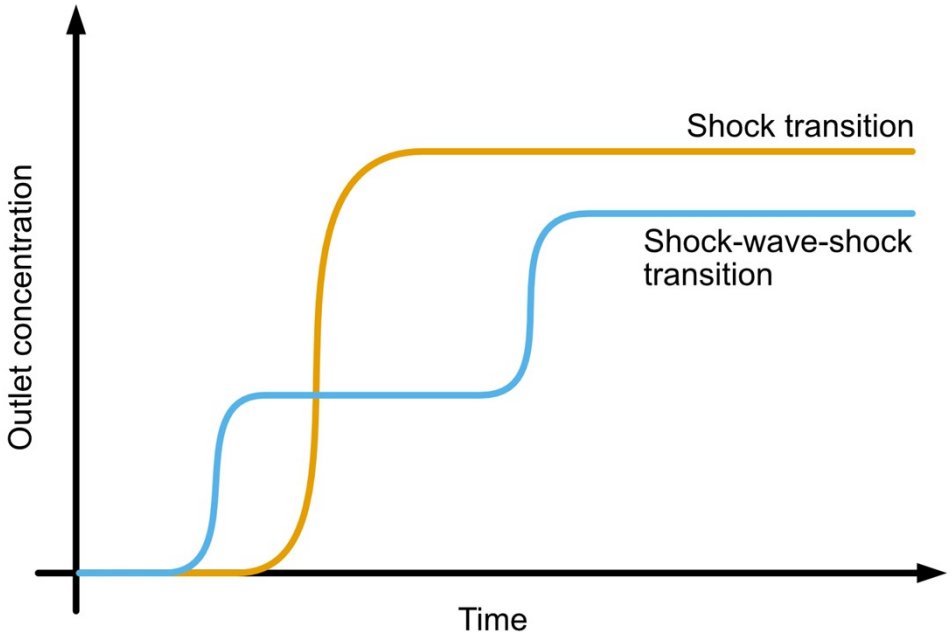

Figure S18. A qualitative demonstration of a shock transition compared to a shock-wave-shock transition.

2. Model description

The model used in this work is an equilibrium adiabatic batch adsorber model. The bed is treated as a well-mixed vessel without any spatial gradients of pressure, temperature, and concentration. Mass transfer resistances are not considered, and the fluid phase is treated as an ideal gas. It is also assumed that the feed step proceeds as a perfect shock-wave until full breakthrough. Competitive adsorption is not estimated for both the stepped isotherm model case, or the dual-site Langmuir case.

Even though most post-combustion CO_2 capture separations are undertaken on an equilibrium basis, the negligence of mass transfer has some implications. Mass transfer rates have an influence on the attainable purity/recovery, and a strong effect on the process productivity.

The adiabaticity is accounted for by splitting each step (stage, in this work) into a series of small pressure increments (300 in this work). For each increment, a mass and energy balance is solved to determine the resulting equilibrium conditions at the new pressure. Enthalpies of adsorption are calculated numerically at each increment. Thermal management is a critical issue for adsorbents with stepped isotherms, as the loading can change suddenly with changes in temperature. However, as the bed temperature is being treated as uniform, accurate propagation of the thermal fronts will not be captured.

The simultaneous equations were solved in MATLAB using *lsqnonlin*, with a central finite difference type, and a function tolerance of 10^{-8}. The initial guess for the gas phase mole fraction of CO_2, and the bed temperature, was the solution from the previous increment. The initial guess for the number of moles added/removed in each increment was zero. A bound was applied to the solution of gas phase mole fraction of CO_2 to be $0 \leq y_A \leq 1$. Temperature and moles of gas added/removed were unbounded, that is, $\pm\infty$.

Calculations are carried out on the basis of 1 kg of adsorbent.

Nomenclature

$C_{P,ads}$ – specific heat capacity of adsorbent [J/kg]
E – total specific energy [J/mol_{CO2}]
ε_{pack} – interparticle packing/void fraction [m^3/m^3]
ε_{pellet} – intraparticle (adsorbent/pellet) void fraction [m^3/m^3]
ε_{total} – total void fraction of the bed (inter- & intraparticle) [m^3/m^3]
η_{isen} – isentropic efficiency [-]
k – adiabatic index (C_P/C_V ratio) [-]
$L_i(P,T,y_i)$ –amount adsorbed of component i as a function of total pressure, temperature, and gas phase mole fraction of i (the isotherm model) [mol/kg]
m – mass of adsorbent [kg]
n_{feed} – total moles fed during the feed/adsorption step [mol]
$n_{raffinate}$ – total moles of raffinate out of the bed during the feed/adsorption step [mol]
n_{tot} – total moles in the system (adsorbent + void space) [mol]
$n_{tot,x}$ – n_{tot} at step/stage x [mol]
n_i – total loading of component i in the system (adsorbent + void space) [mol]
$n_{i,x}$ – n_i at step/stage x [mol]
P – total pressure [bar_a]
P_{ads} – adsorption pressure [bar_a]
P_{atm} – atmospheric pressure (1.01325 bar_a) [bar_a]

P_i – partial pressure of component i ($P \times y_i$) [bar_a]
$Q_i(P,T,y_i)$ – heat of adsorption of component i as a function of total pressure, temperature, and gas phase mole fraction of i [J/mol]
R – universal gas constant [J/mol/K]
ρ_{bed} – packed bed (bulk) density [kg/m^3]
ρ_{pellet} – particle (envelope) density [kg/m^3]
T – temperature [K]
T_{ads} – adsorption temperature [K]
V_{void} – total volume of the bed void space (inter- and intra-particle voids) [m^3]
W_{feed} – feed compression work [J]
W_{vac} – vacuum pump work [J]
$W_{vac,x}$ – total vacuum pump work in step/stage x [J]
y_a – gas phase mole fraction of the heavy component (CO_2 in this case) [i]
y_b – gas phase mole fraction of the light component (N_2 in this case) [i]
y_i – gas phase mole fraction of component i [i]
$y_{i,x}$ – y_i at step/stage x [-]
y_{LP} – gas phase CO_2 mole fraction in the light product (raffinate) [-]

2.1. Constants

The packing void fraction of the bed (ε_{pack}) is assumed to be 0.37, and the total void space is given by:

$$\varepsilon_{tot} = \varepsilon_{pack} + \left(1 - \varepsilon_{pack}\right) \cdot \varepsilon_{pellet}$$

The density of the bed is given by:

$$\rho_{bed} = \left(1 - \varepsilon_{pack}\right) \cdot \rho_{pellet}$$

The total void space of the bed is then given by:

$$V_{void} = \frac{m}{\rho_{bed}} \cdot \varepsilon_{tot}$$

Isentropic efficiencies (η_{isen}) of compressors and vacuum pumps are assumed to be 0.83.

2.2. Initial conditions (step/stage 0)

The bed is at equilibrium with the feed gas conditions.

$$y_{a,0} = y_{a,feed} \qquad y_{b,0} = 1 - y_{a,0}$$

$$n_{i,0} = L_i\left(P_{ads}, T_{ads}, y_{i,0}\right) \cdot m + \frac{P_{ads} \cdot y_{i,0} \cdot V_{void}}{R \cdot T_{ads}}, \qquad i = \{a,b\}$$

$$n_{tot,0} = n_{a,0} + n_{b,0}$$

2.3. Blowdown step (step/stage 1)

The pressure (P) is reduced from the adsorption pressure (P_{ads}) to the blowdown pressure (P_{BD}) in a series of small increments. The heat of adsorption is calculated first at the current temperature, pressure, and gas phase composition. In the case of F4_MIL-140A(Ce) where the specific heat capacity is not a constant value, it is also calculated first at the current temperature.

The mass and energy balances are solved simultaneous for the gas phase mole fraction of y_a (x_1), total moles removed from the bed at composition x_1 (x_2), and temperature (x_3). The subscript "prev" signifies the result from the previous increment (or, the current conditions in the bed before the next increment is carried out).

$$n_{a,prev} - x_1 \cdot x_2 = L_a\left(P, x_3, x_1\right) \cdot m + \frac{P \cdot x_1 \cdot V_{void}}{R \cdot x_3}$$

$$n_{b,prev} - \left(1 - x_1\right) \cdot x_2 = L_b\left(P, x_3, 1 - x_1\right) \cdot m + \frac{P \cdot \left(1 - x_1\right) \cdot V_{void}}{R \cdot x_3}$$

$$x_3 = T_{prev} + \frac{Q_a\left[L_a\left(P, x_3, x_1\right) - L_{a,prev}\right] + Q_b\left[L_b\left(P, x_3, 1 - x_1\right) - L_{b,prev}\right]}{C_{P,ads}}$$

The total moles removed during the blowdown step are given by summing x_2 over the series of small increments.

If P is below P_{atm}, vacuum work is calculated according to the following:

$$W_{vac} = x_2 \cdot \frac{R \cdot x_3}{\eta_{isen}}\left(\frac{k}{k-1}\right)\left[\left(\frac{P_{atm}}{P}\right)^{\frac{k-1}{k}} - 1\right]$$

Where k is the adiabatic index (C_P/C_V ratio) of the gas (see Section 2.10).

The total vacuum work required for the step are given by summing W_{vac} over the series of small increments.

2.4. Depressurisation (step/stage 2)

This step is calculated in the same way as the blowdown step, except for pressures between the blowdown pressure (P_{BD}) and the desorption pressure (P_{des}).

The gas removed from this step is the CO_2 product gas. The purity of the CO_2 product is given by the ratio of the amount of CO_2 removed to the total amount of gas removed.

$$\text{Purity} = \frac{n_{CO_2,2}}{n_{CO_2,2} + n_{N_2,2}}$$

2.5. Light-product pressurisation (step/stage 3)

This step is carried out between the desorption pressure (P_{des}) and the adsorption pressure (P_{ads}).

Due to perfect shock-wave assumption for the feed step, the composition of the light product gas is equal to the composition of the gas phase at the end of the pressurisation (this) step. Consequently, this step is solved iteratively.

First, it is assumed that the CO_2 concentration in the light product (y_{LP}) is 1 %. For this step, x_2 represents the moles of light product added to the bed.

$$n_{a,prev} + y_{LP} \cdot x_2 = L_a\left(P, x_3, x_1\right) \cdot m + \frac{P \cdot x_1 \cdot V_{void}}{R \cdot x_3}$$

$$n_{b,prev} + \left(1 - y_{LP}\right) \cdot x_2 = L_b\left(P, x_3, 1 - x_1\right) \cdot m + \frac{P \cdot \left(1 - x_1\right) \cdot V_{void}}{R \cdot x_3}$$

$$x_3 = T_{prev} + \frac{Q_a\left[L_a\left(P, x_3, x_1\right) - L_{a,prev}\right] + Q_b\left[L_b\left(P, x_3, 1 - x_1\right) - L_{b,prev}\right]}{C_{P,ads}}$$

Once P_{ads} is reached (last increment), the value of x_1 is compared to y_{LP}. If they are within 0.01 %, there are no further iterations. If they are not within 0.01 %, the calculation is looped (starting from the end of the depressurisation step) with a new value of y_{LP} equal to the value of x_1.

2.6. Feed (step/stage 4)

The feed step is treated as a mass balance to achieve 'cyclic steady state'. That is, how much feed gas is required to go from the state at the end of the light-product pressurisation step to the initial conditions.

$$n_{a,0} = n_{a,3} + n_{feed} \cdot y_{a,feed} - n_{raffinate} \cdot y_{LP}$$

$$n_{b,0} = n_{b,3} + n_{feed} \cdot \left(1 - y_{a,feed}\right) - n_{raffinate} \cdot \left(1 - y_{LP}\right)$$

In this situation, n_{feed} and $n_{raffinate}$ are the only unknowns. The linear equations are solved simultaneously.

Once n_{feed} is known, the recovery of the process can be calculated from the ratio of CO_2 recovered in the depressurisation step and the CO_2 fed in the feed step.

$$\text{Recovery} = \frac{n_{CO_2,2}}{n_{feed} \cdot y_{a,feed}}$$

2.7. Enthalpy of adsorption calculation

As competitive adsorption is not being accounted for in this work, the heat of adsorption can be given by[4]:

$$Q_i = \frac{RT^2}{P_i}\frac{\partial L_i/\partial T}{\partial L_i/\partial P_i}$$

For the numerical evaluation of the derivatives, a ΔT of 1×10^{-3} K, and a ΔP_i of 1×10^{-6} bar was used.

$$Q_i \cong \frac{RT^2}{P_i}\cdot\frac{\dfrac{L_i(P,T+\Delta T,y_i)-L_i(P,T-\Delta T,y_i)}{2\cdot\Delta T}}{\dfrac{L_i(P+\Delta P,T,y_i)-L_i(P-\Delta P,T,y_i)}{2\cdot\Delta P}}$$

2.8. Feed compression calculation

As feed pressurisation is considered in this work, it is necessary to account for the potential multi-stage compression of the feed.

This is carried out iteratively by adding compression stages until the required pressure ratio (PR) between stages is ≤ 2. Iteration is required in this instance because the pressure drop of the interstage cooling (ΔP_{HX}) is taken into consideration. It is assumed to be 0.2 bar.

The pressure after compression stage N (P_N) is given by:

$$P_N = P_{N-1}\cdot PR - \Delta P_{HX}$$

First, 1 stage is assumed to be sufficient, and PR calculated using *fsolve* in MATLAB (with default options).

If the resulting PR is > 2, another stage is added by looping the output pressure calculation N times.

Once the number of stages (N_S) and pressure ratio is determined to achieve the desired P_{ads}, the specific compression work per stage ($\hat{W}_N$) can be calculated with the following:

$$P_N = P_{N-1}\cdot PR - \Delta P_{HX}$$

$$\hat{W}_N = \frac{RT_{feed}}{\eta_{isen}}\frac{k}{k-1}\left[PR^{\frac{k-1}{k}}-1\right]$$

It is assumed that the temperature is reduced to the feed gas temperature (temperature at which flue gas is supplied to the process, not the adsorption temperature) after inter-stage cooling. The value of the adiabatic index (k) is calculated for each stage at its feed pressure.

The total feed compression work (W_{feed}) is then given by:

$$W_{feed} = n_{feed}\sum_{N=1}^{N_S}\hat{W}_N$$

2.9. Specific energy calculation

The total specific energy (J/mol_{CO2}) is determined based on the vacuum work calculated in sections 2.3 and 2.4, and the feed compression energy requirements from section 2.8. The CO_2 product is based on the amount of CO_2 collected during step 2 (section 2.4).

Specifically:

$$E = \frac{W_{vac,1} + W_{vac,2} + W_{feed}}{n_{CO_2,2}}$$

2.10. Adiabatic index

The function to determine the adiabatic index (heat capacity ratio) of the feed gas was required to be updated for this work. The original function in our previous work only covered a range of 1 to 200 kPa_a, and 20 to 100 °C.[7]

New adiabatic index data was generated in ASPEN HYSYS using the Peng-Robinson fluid package covering a range of 1 to 1000 kPa_a, 0 to 100 °C. The numerical data was then fit in ALAMO.[8]

The fitted function is:

$$k = 16.88660981 \cdot \tau + 2.1\times10^{-6} \cdot P + 1.127420548 \cdot C + 1.344335014 \cdot N - 0.000151 \cdot \ln(P) + \text{K}$$
$$0.0826 \cdot C^2 - 0.0181 \cdot C^3 + 0.00583 \cdot \tau P + 8.443063659 \cdot \tau C - 0.000129 \cdot PC - 0.000983 \cdot (\tau P)^2 + \text{K}$$
$$0.000204 \cdot (\tau P)^3 + 0.0525 \cdot \tau PC + 2.535102164 \cdot \tau CN - 4.87\times10^{-6} \cdot PCN + 0.000578 \cdot (\tau PC)^2$$

Where:

$$\tau = \frac{1}{T}$$
$$C = y_{CO2}$$
$$N = y_{N2} = (1 - y_{CO2})$$

With T in Kelvin, and P in kPa.

The goodness of fit is shown below in Figure S19.

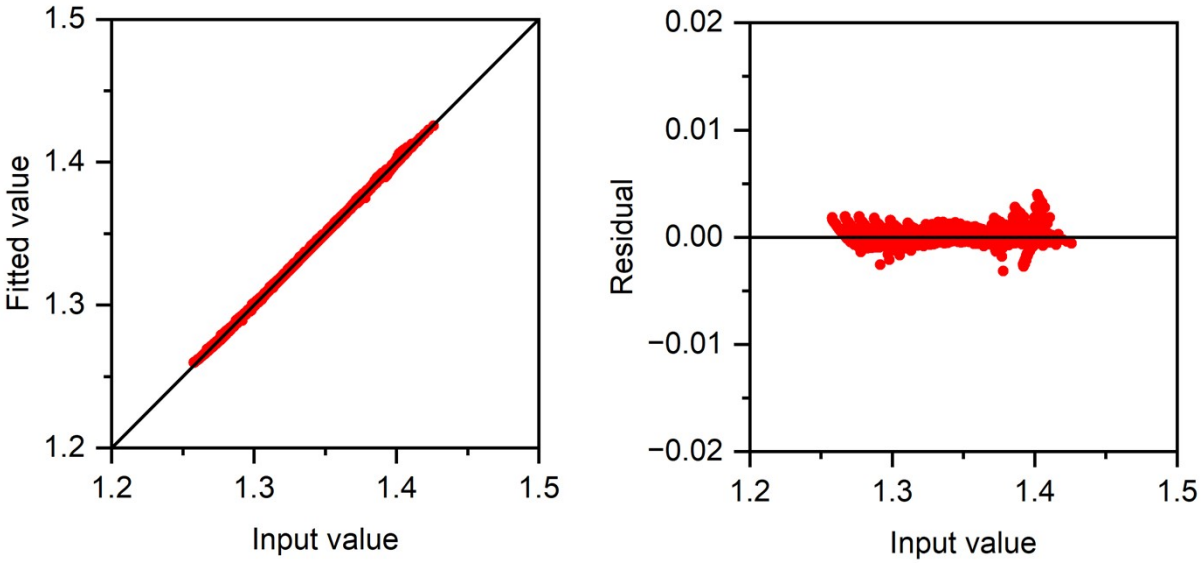

Figure S19: Parity plot (left) and residuals plot (right) of adiabatic index surrogate model fitting.

3. Adsorbent isotherm parameters and properties

This section contains the input data for the adsorbents evaluated including the: isotherm fitting parameters, physical properties, and any data sources.

3.1. F4_MIL-140A(Ce)

Units are as follows: T_0 – K, $p_{step,0}$ – bar, H_{step} – J·mol^{-1}, n_i^{∞} – mol·kg^{-1}, b_i^{∞} – bar^{-1}, E_i – J·mol^{-1}, ρ – kg·m^{-3}, ε – m^3·m^{-3}, C_P – J·kg^{-1}·K^{-1}. χ and γ are unitless.

Isotherm parameters			
CO_2			
T_0	2.5315×10^{2}	**E_L**	3.9772×10^{4}
$p_{step,0}$	7.5420×10^{-3}	**n_U^{∞}**	2.6572×10^{0}
H_{step}	3.9776×10^{4}	**b_U^{∞}**	3.3204×10^{-7}
χ_1	1.2330×10^{-2}	**E_U**	4.2735×10^{4}
χ_2	6.6055×10^{2}	**b_H^{∞}**	1.3344×10^{-3}
n_L^{∞}	1.5020×10^{2}	**E_H**	4.1670×10^{3}
b_L^{∞}	1.6174×10^{-9}	**γ**	4.6714×10^{-1}
N_2			
T_0	2.5315×10^{2}	**E_L**	4.2444×10^{4}
$p_{step,0}$	7.1356×10^{-1}	**n_U^{∞}**	2.4511×10^{-1}
H_{step}	0.0000×10^{0}	**b_U^{∞}**	3.0922×10^{-10}
χ_1	1.0053×10^{0}	**E_U**	6.2986×10^{4}
χ_2	0.0000×10^{0}	**b_H^{∞}**	1.1786×10^{-5}
n_L^{∞}	1.1810×10^{1}	**E_H**	0.0000×10^{0}
b_L^{∞}	1.2135×10^{-10}	**γ**	5.6688×10^{0}

Physical properties	
Density	1046
Porosity	0.54
CIF file source	CCDC: WOTVOT
Heat capacity	$C_P = 1.75604\times T + 274.13055$ Where T is in K.

3.2. Other adsorbents

Units are as follows: m – $mol \cdot kg^{-1}$, b_0 – bar^{-1}, ΔH – $J \cdot mol^{-1}$, ρ – $kg \cdot m^{-3}$, ε – $m^3 \cdot m^{-3}$, C_p – $J \cdot kg^{-1} \cdot K^{-1}$

	HKUST-1	UTSA-16	Activated carbon	13X	CALF-20
Isotherm parameters					
CO_2					
m_1	5.9751×10^{4}	4.0790×10^{0}	2.2390×10^{0}	3.7919×10^{0}	2.4484×10^{0}
$b_{0,1}$	8.2574×10^{-7}	6.0000×10^{-6}	1.8072×10^{-5}	1.2313×10^{-8}	1.2214×10^{-5}
ΔH_1	1.9618×10^{2}	3.4250×10^{4}	2.9177×10^{4}	5.3350×10^{4}	3.6439×10^{4}
m_2	1.3274×10^{1}	1.2890×10^{0}	3.2259×10^{0}	3.8477×10^{0}	2.5937×10^{0}
$b_{0,2}$	5.7224×10^{-7}	1.6260×10^{-8}	2.2957×10^{-6}	9.0542×10^{-12}	4.4948×10^{-10}
ΔH_2	3.4554×10^{4}	3.7820×10^{4}	2.8980×10^{4}	5.9698×10^{4}	5.0609×10^{4}
N_2					
m_1	5.9143×10^{0}	1.3260×10^{0}	1.7095×10^{0}	3.3240×10^{0}	2.6640×10^{0}
$b_{0,1}$	9.5120×10^{-5}	2.1540×10^{-3}	2.1228×10^{-4}	4.9072×10^{-5}	2.0956×10^{-5}
ΔH_1	1.5364×10^{4}	8.5580×10^{3}	1.7077×10^{4}	1.8305×10^{4}	2.1244×10^{4}
m_2	-	1.7730×10^{0}	4.9931×10^{-1}	1.7998×10^{1}	-
$b_{0,2}$	-	1.6690×10^{-7}	4.7536×10^{-4}	2.6079×10^{-5}	-
ΔH_2	-	3.0280×10^{4}	1.1232×10^{4}	1.0844×10^{4}	-
Isotherm data source	1	2	3	5	6
Digitised data	Yes	No	No	No	No

Physical properties					
Density	446	787	480.5	750	340
Porosity	0.81	0.61	0.69	0.71	0.61
CIF file source	CCDC: DOTSOV42	CCDC: RAZXIA	-	[4]	[6]
C_p	803	878	1050	920	1371
C_p source	-	-	[4]	[4]	[6]

4. Simulated adsorption isotherms

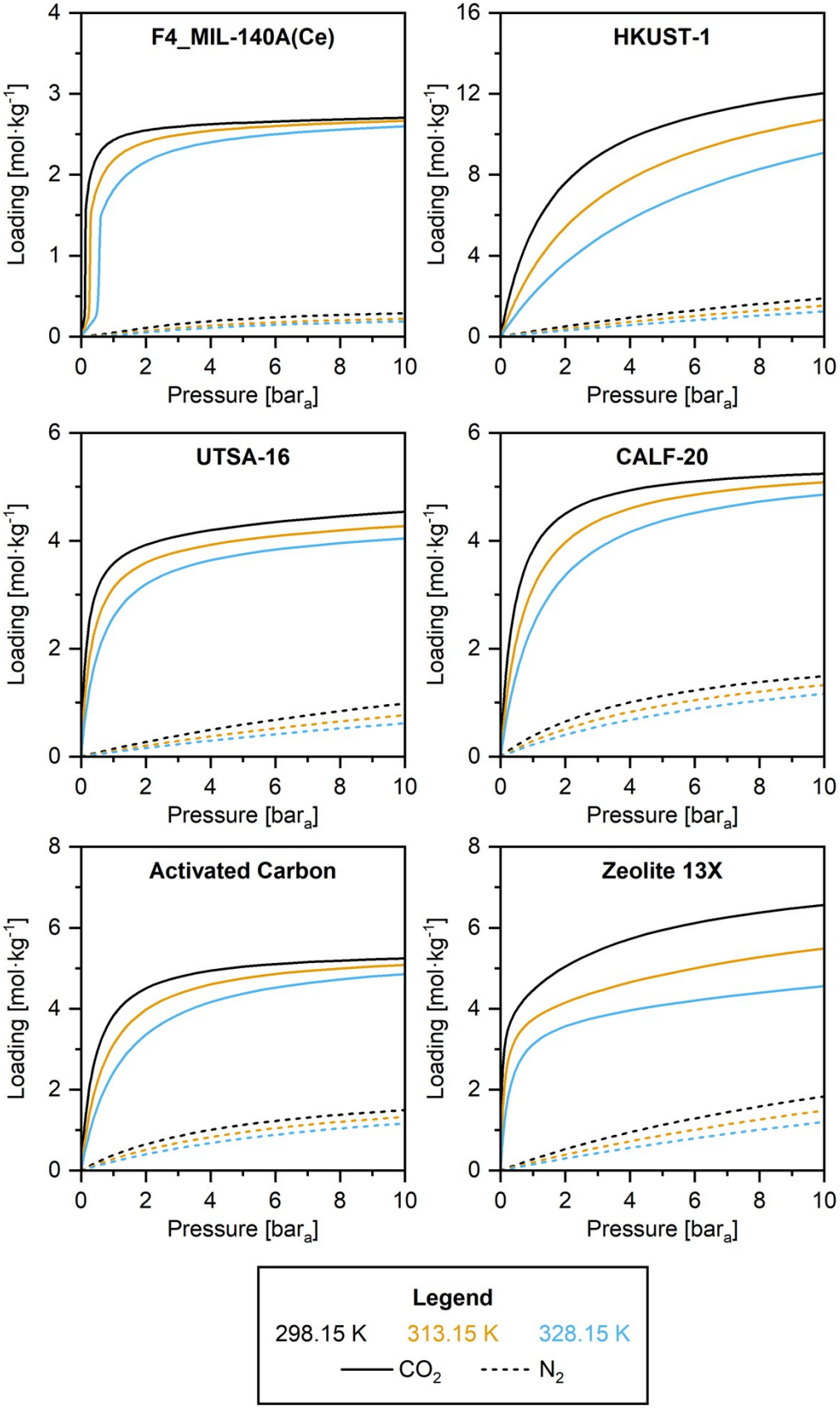

Figure S20: Representative isotherms of the adsorbents studied in this work, generated from the fitting parameters of Section 3.

5. Specific energy consumption

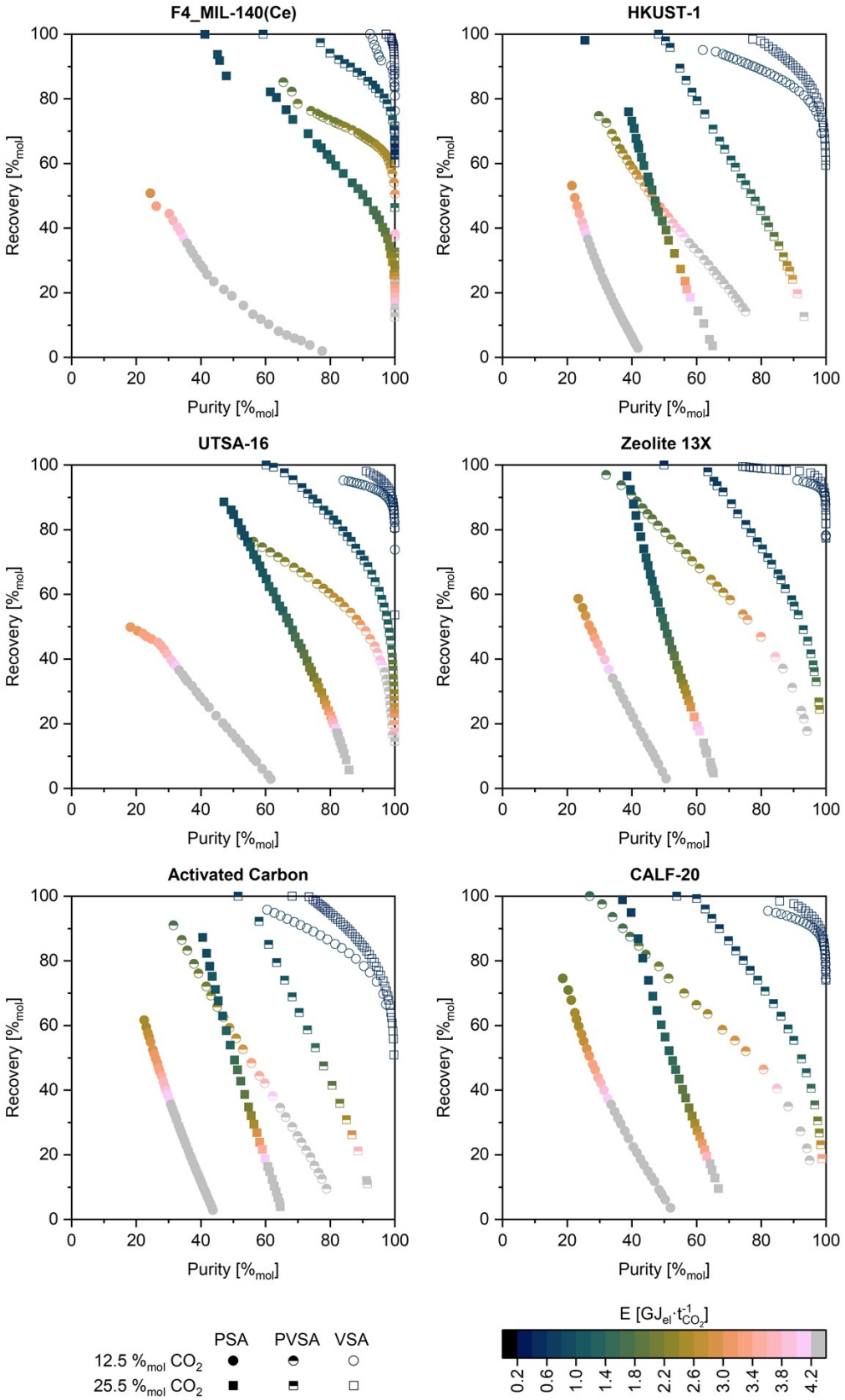

Figure S21: Purity-recovery Pareto fronts for each adsorbent, colour-mapped by specific energy consumption (electrical). The symbol shape and fill style represent the flue-gas CO_2 concentration and cycle type, respectively.

6. Supplementary references

1 Z. Liang, M. Marshall and A. L. Chaffee, *Energy Fuels*, 2009, **23**, 2785–2789.
2 V. I. Agueda, J. A. Delgado, M. A. Uguina, P. Brea, A. I. Spjelkavik, R. Blom and C. Grande, *Chem. Eng. Sci.*, 2015, **124**, 159–169.
3 F. V. S. Lopes, C. A. Grande, A. M. Ribeiro, J. M. Loureiro, O. Evaggelos, V. Nikolakis and A. E. Rodrigues, *Sep. Sci. Technol.*, 2009, **44**, 1045–1073.
4 B. J. Maring and P. A. Webley, *Int. J. of Greenh. Gas Control*, 2013, **15**, 16–31.
5 S. Cavenati, C. A. Grande and A. E. Rodrigues, *J. Chem. Eng. Data*, 2004, **49**, 1095–1101.
6 T. T. T. Nguyen, J.-B. Lin, G. K. H. Shimizu and A. Rajendran, *Chem. Eng. J.*, 2022, **442**, 136263.
7 D. Danaci, M. Bui, N. Mac Dowell and C. Petit, *Mol. Syst. Des. Eng.*, 2020, **5**, 212–231.
8 Z. T. Wilson and N. V. Sahinidis, *Comput. Chem. Eng.*, 2017, **106**, 785–795.